

# Some Remarkable Properties of a Hopfield Neural Network with Time Delay

Kelvin Rozier, Vladimir E. Bondarenko

**Abstract**—It is known that an analog Hopfield neural network with time delay can generate the outputs which are similar to the human electroencephalogram. To gain deeper insights into the mechanisms of rhythm generation by the Hopfield neural networks and to study the effects of noise on their activities, we investigated the behaviors of the networks with symmetric and asymmetric interneuron connections. The neural network under the study consists of 10 identical neurons. For symmetric (fully connected) networks all interneuron connections  $a_{ij} = +1$ ; the interneuron connections for asymmetric networks form an upper triangular matrix with non-zero entries  $a_{ij} = +1$ . The behavior of the network is described by 10 differential equations, which are solved numerically. The results of simulations demonstrate some remarkable properties of a Hopfield neural network, such as linear growth of outputs, dependence of synchronization properties on the connection type, huge amplification of oscillation by the external uniform noise, and the capability of the neural network to transform one type of noise to another.

**Keywords**—Chaos, Hopfield neural network, noise, synchronization

## I. INTRODUCTION

CHAOTIC neural networks are subjects of intensive investigations during the last several decades [1]. Different aspects of the chaotic neural network behavior were studied, such as their stability properties [2], conditions for synchronization [3], generation of different types of chaotic activities [4], and information processing [5]. In particular, significant attention is paid to the Hopfield neural networks with time delays, which can produce chaotic activity similar to the human or animal electroencephalogram (EEG) [6]-[8]. It was shown that such a neural network can generate activities with the correlation dimensions and the largest Lyapunov exponents, which are close to those obtained from the human EEG analysis [6], [7]. Due to this fact and that these neural nets were useful in testing methods of the human EEG analysis they have been called “synthetic brains” [9], [10].

While a number of different studies of the Hopfield neural networks have been performed, there has been little attention to the variety of different types of activities generated by Hopfield neural networks. In this paper, we consider relatively simple analog Hopfield neural networks with excitatory connections and fixed time delay. We found that the Hopfield neural network shows several remarkable properties depending on the type of the connection matrix (symmetric or asymmetric) and the connection strength.

This work was supported in part by a grant from American Heart Association 10GRNT4720012 and a Research Initiation Grant from Georgia State University to V. E. Bondarenko.

K. Rozier is a graduate student in the Department of Mathematics and Statistics, Georgia State University, Atlanta, GA 30303 USA (e-mail: krozier3@student.gsu.edu).

V. E. Bondarenko is with the Department of Mathematics and Statistics, Georgia State University, Atlanta, GA 30303 USA (corresponding author; phone: 404-413-6440; fax: 404-413-6403; e-mail: vbondarenko@gsu.edu).

These properties include complete synchronization in time and amplitudes, synchronization in time only, decaying and growing output amplitudes, including unusual linear growth of the output amplitude. We also show that the application of uniform noise to the Hopfield neural network under one of the above-mentioned regimes produced irregular behavior with different properties. Finally, we demonstrated that this neural network with applied noise can significantly amplify low-amplitude oscillations.

## II. METHODS

An analog Hopfield neural network with time delay is described by the set of ordinary differential equations [6]:

$$\dot{u}_i(t) = -u_i(t) + \sum_{j=1}^M a_{ij} f(u_j(t-\tau)) + d\xi(t),$$

where  $u_i(t)$  is the input of the  $i^{\text{th}}$  neuron,  $a_{ij}$  is the connectivity matrix,  $\tau$  is the time delay of the  $j^{\text{th}}$  neuron,  $f(x) = c \tanh(x)$ ,  $i, j = 1, 2, \dots, M$ ,  $c$  is the coupling strength,  $\xi(t)$  is the external uniform noise, which varies in the interval  $[-1, +1]$ ,  $\langle \xi(t) \rangle = 0$ , and  $d$  is the noise amplitude. We studied the neural network with ten neurons ( $M = 10$ ) and the fixed value of time delay  $\tau = 10.0$ . The model equations were solved by the 4<sup>th</sup> order Runge-Kutta method with dimensionless time step 0.1. Very small random values of  $u_i(0)$  in the interval  $[-2 \cdot 10^{-100}, 2 \cdot 10^{-100}]$  were used as initial conditions. For the time  $t$  in the interval from  $-\tau$  to less than 0 all  $u_i = 0$ . Total length of the simulated time series were equal to  $N = 2^{18} = 262,144$  of dimensionless units. The neural network model was implemented as C++ code which was run on a 64-bit operating system.

In this paper, we studied neural networks with the coefficients  $a_{ij} = +1$  for all  $i, j = 1, 2, \dots, M$  (fully connected neural network, or symmetric neural network) and  $a_{ij} = +1$  for all  $i = 1, 2, \dots, M$  and  $j = i, \dots, M$  (neural network with an upper triangular matrix of connections, or asymmetric neural network). Using an upper triangular matrix allows for investigation of the effects of asymmetry on the neural network dynamics. In simulations, the coefficient  $c$  was varied from 0.01 to 10.0.

To calculate the amplitude distribution function for time series  $\{u_i\}$ ,  $i = 1, 2, \dots, N$ , obtained in this study on the fixed interval  $[u_{\min}, u_{\max}]$  we divide this interval into 128 subintervals with length  $\Delta = (u_{\max} - u_{\min})/128$ . Then, for each subinterval, we calculated the number of  $u_i$ , which fall into a subinterval. In addition, we evaluated the energy function  $E$  according to the equation:

$$E = \frac{1}{N} \sum_{i=1}^N \left( \frac{u_i - \bar{u}}{A} \right)^2,$$

where

$$\bar{u} = \frac{1}{N} \sum_{i=1}^N u_i$$

is the average value of  $\{u_i\}$ ,  $A$  is the normalization constant.

To compare shapes of the amplitude distribution functions for the time series that varies in wide range of amplitudes, we also calculated the normalized amplitude distribution function, using 128 normalized subintervals:

$$\Delta_n = 4\sqrt{E\Delta}$$

### III. RESULTS

#### A. Hopfield Neural Networks without Noise

First we investigated the behavior of the Hopfield neural networks without an external noise. Fig. 1 shows the time behavior of the neural outputs in a fully connected neural network. There are two different types of the network's behavior, depending on the value of the coupling strength  $c$ . When  $c < c_{th}$  (Fig. 1A;  $c_{th} \approx 0.103$  is the threshold value of  $c$ , when decaying neural outputs transform into growing outputs), we observe initial decay of the neural output amplitudes from the initial conditions. At the time moment  $t = 10.0$  all decaying outputs become completely synchronized, both in time and in amplitude (Fig. 1A).

At the larger (suprathreshold) value of  $c = 1.0$ , initially decaying neural outputs become growing outputs in time (Fig. 1B). As in the case of subthreshold activity, the outputs are fully synchronized, both in time and in amplitude. The growing amplitudes increase until saturation (Fig. 1C) at the values of  $u_i = M \times c$  ( $10 \times 1.0 = 10.0$ ), which is typical behavior for the unstable nonlinear system. The neural outputs also contain growing oscillations, which are superimposed with an exponentially growing component of the neural outputs (Fig. 1D). The oscillation quasi-period is approximately equal to the time delay  $\tau = 10.0$  in dimensionless units. Once saturating values of the neural outputs are reached the oscillations cease.

To investigate the effects of asymmetry on the neural network dynamics, we used an upper triangular connectivity matrix  $a_{ij}$ . Incorporation of asymmetry remarkably changed the neural network dynamics. At subthreshold values of  $c = 0.1$  ( $c < c_{th} \approx 0.996$ ; Fig. 2A), the neural network outputs first decay from their initial values. Then, at  $t = 10.0$ , the outputs become decaying oscillations, which are synchronized, however, in time only (compare to outputs in Fig. 1A of the fully connected neural network).

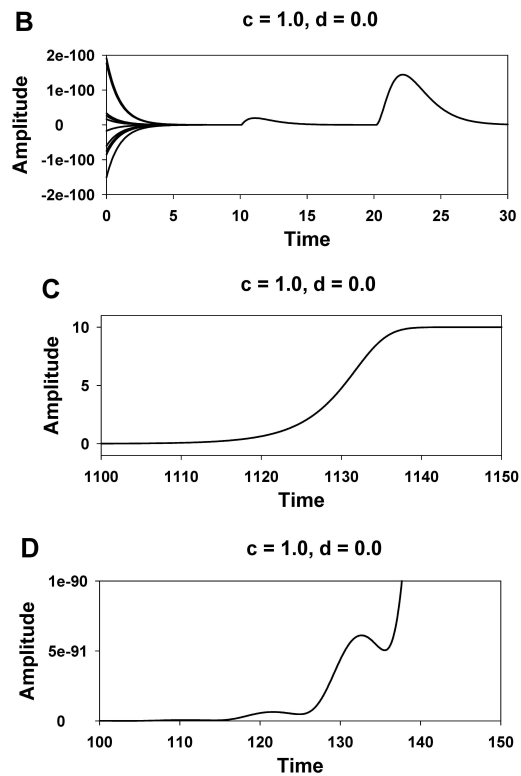
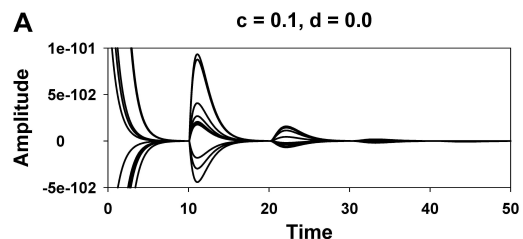
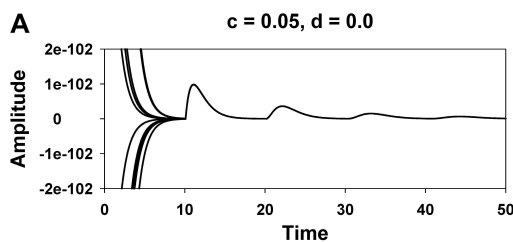


Fig. 1 Activity of the fully connected neural network with  $a_{ij} = 1$  and without noise ( $d = 0.0$ ). (A) Subthreshold case ( $c = 0.05$ ). Decaying oscillations. (B) Suprathreshold case ( $c = 1.0$ ). Growing oscillations. (C) Suprathreshold case ( $c = 1.0$ ). Growing amplitudes saturate. (D) Suprathreshold case ( $c = 1.0$ ). Oscillatory activity of the neural network is superimposed with an exponentially growing component

When  $c = 1.0 > c_{th}$ , the neural outputs represent growing oscillations (Fig. 2B). As in the case of subthreshold activity, the neural outputs have different magnitudes and are synchronized in time only. Fig. 2C demonstrates typical suprathreshold activity of the neural network with an upper triangular connectivity matrix. This includes three major stages: 1) exponential growth, which is typical for the most unstable nonlinear systems; 2) unusual linearly growing neural network outputs (see Fig. 2D for details); and 3) saturation, which is also often observed in many nonlinear dynamical systems. In addition, the threshold value  $c_{th}$  for the neural network with the upper triangular connectivity matrix is significantly (by a factor of  $\sim 10$ ) greater compared to the fully connected network, pointing to the stabilizing effect of the asymmetry of interneuron connections.



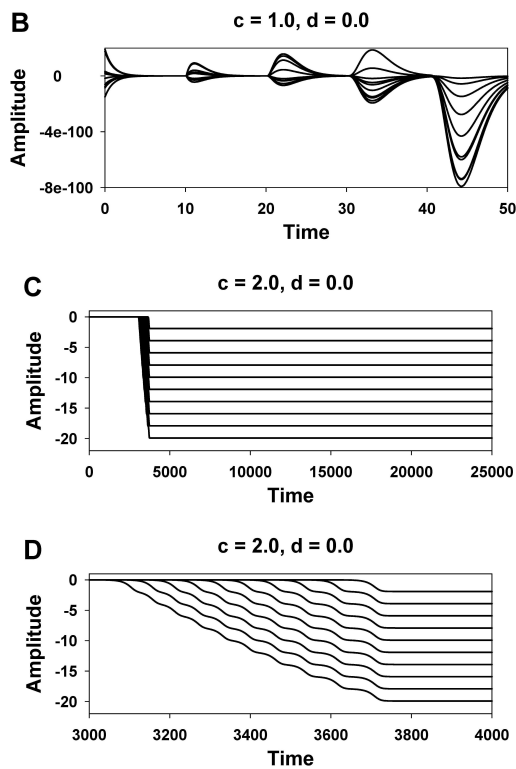


Fig. 2 Activity of the neural network with upper triangular connectivity matrix  $a_{ij}$  and without noise ( $d = 0.0$ ). (A) Subthreshold case ( $c = 0.1$ ). Decaying oscillations. (B) Suprathreshold case ( $c = 1.0$ ). Growing oscillations. (C) Suprathreshold case ( $c = 2.0$ ). Growing amplitudes saturate; an interval of linear growth is observed. (D) Suprathreshold case ( $c = 2.0$ ). Closer look at the linearly growing neural network outputs

### B. Hopfield Neural Networks with Noise

We also studied the effects of uniform noise on the activity of a fully connected Hopfield neural network and a neural network with an upper triangular connectivity matrix. The noise was generated by a random number generator, which produced uniformly distributed amplitudes on the interval  $[-1, 1]$ . Fig. 3A shows the initial part of the time series of uniform noise used in this study, and the amplitude distribution diagram is shown in Fig. 3B. The noise time series of 262,144 points is used for the calculation of the diagram. The interval  $[-1, 1]$  was divided into 128 subintervals with the length  $\Delta = 2/128 = 0.015625$ , and the number of points in each subinterval was calculated. The distribution diagram for the amplitudes of uniform noise plotted in Fig. 3B clearly show their good uniform distribution.

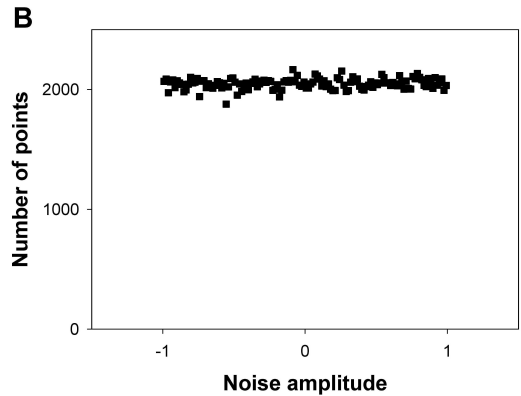
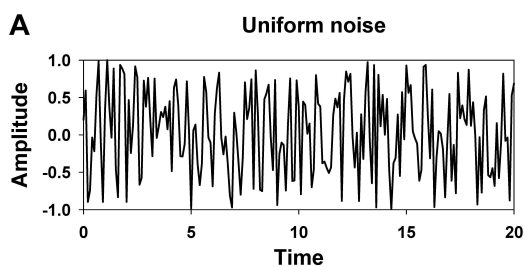


Fig. 3 (A) Time series of the external uniform noise  $\xi(t)$ . Only first 200 points are shown. (B) Amplitude distribution diagram for uniform noise calculated from times series of 262,144 points

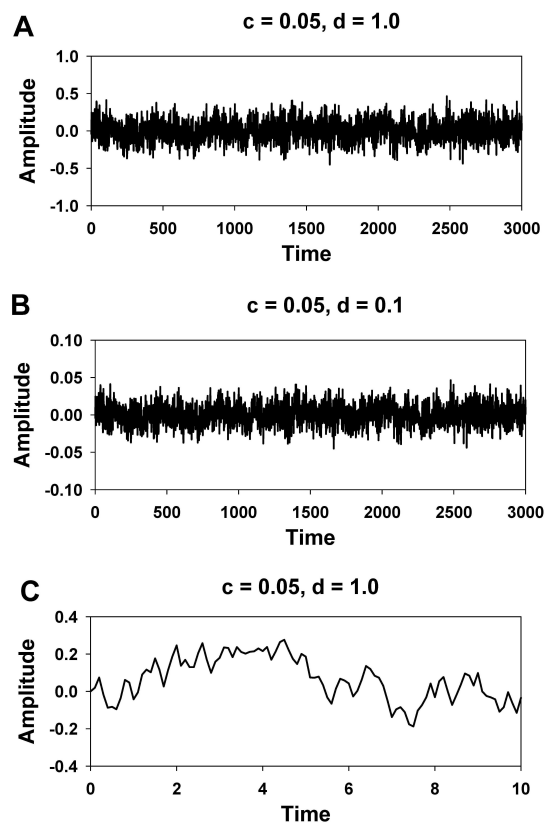


Fig. 4 Neural network outputs under influence of external noise ( $c = 0.05$  (subthreshold case, fully connected neural network);  $d = 1.0$  (A) and  $d = 0.1$  (B)). Panel C shows details of fully synchronous activity from panel A

We first studied the effects of noise on a fully connected Hopfield neural network at  $c = 0.05$  (subthreshold case). Fig. 4A shows neural network outputs under the effects of a uniform noise (noise amplitude  $d = 1.0$ ). It is interesting to note that the neural output amplitudes vary in significantly smaller intervals than the amplitude of applied noise (compare Figs. 4A and 3A). At smaller magnitudes of the applied noise ( $d = 0.1$ ), the neural outputs also show smaller amplitudes (Fig. 4B). Another interesting property of the neural network

activity is that all neurons in the network demonstrate synchronous behavior since the very first time moment, once the noise is applied (Fig. 4C).

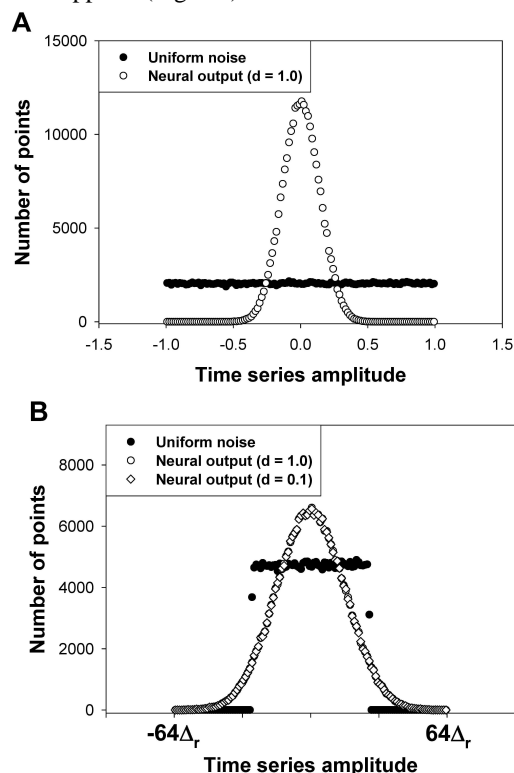


Fig. 5 Amplitude distribution functions (A) and normalized amplitude distribution functions (B) for the neural network outputs under influence of the external noise and for amplitudes of the external noise ( $c = 0.05$ , subthreshold case of the fully connected neural network)

It is remarkable that the Hopfield neural network transforms properties of the external uniform noise. This transformation is illustrated by Fig. 5. Fig. 5A shows two amplitude distributions, one is for uniform noise (filled circles) and another is for neural network outputs for all 10 neurons (unfilled circles,  $d = 1.0$ ). The noise amplitude is distributed uniformly on the interval  $[-1, 1]$ , while the distribution of the amplitudes of neural outputs at the noise amplitude  $d = 1.0$  is bell-shaped (Fig. 5A). At smaller values of  $d = 0.1$ , neural network outputs have smaller magnitudes (Fig. 4B). Due to small amplitudes, the distribution function for this case has non-zero values only in a few subintervals about zero (data not shown). To obtain amplitude distribution functions, which are not strictly bound to the frame on the interval  $[-1, 1]$ , we employed calculations of the normalized amplitude distribution function, as described in the Methods section. The normalized amplitude distribution functions for uniform noise and for neural network outputs at  $d = 1.0$  and  $d = 0.1$  are shown in Fig. 5B. The uniform noise has a rectangular distribution function, while both neural network outputs show bell-shaped distributions. Note that despite the 10-fold difference in neural output amplitudes (Fig. 4, A and B), their normalized distribution functions are very similar (unfilled circles and unfilled diamonds in Fig. 5B).

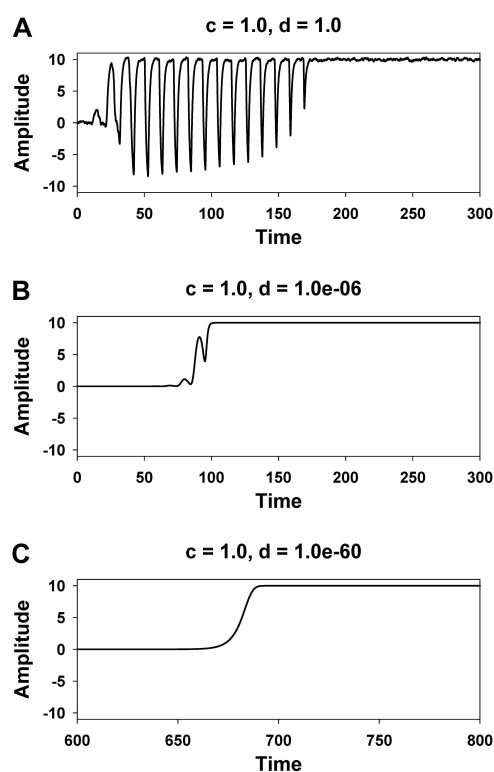


Fig. 6 The activity of the fully connected neural network with external noise. Suprathreshold case ( $c = 1.0$ ); external noise amplitudes are  $d = 1.0$  (A),  $d = 1.0 \times 10^{-6}$  (B), and  $d = 1.0 \times 10^{-60}$  (C)

We also investigated the effects of external uniform noise on a fully connected Hopfield neural network at suprathreshold values of  $c$ . Similar to the case when noise is absent, the neural network outputs increase in magnitudes until saturation, and the neural outputs are fully synchronized (Fig. 6). There are two major effects of noise on the network activity: a decrease of the time interval to the output saturation and huge transient amplification of the oscillatory component. Fig. 6A shows transient large-amplitude oscillations, which become visible on the increasing part of the neural outputs in the presence of noise (noise amplitude is  $d = 1.0$ ; compare with small-amplitude oscillations in Fig. 1D where  $d = 0.0$ ). In this case, the neural network acts as a powerful amplifier that can increase oscillation amplitude by approximately 90 orders of magnitude. Even relatively small noise with  $d = 1.0 \times 10^{-6}$  can remarkably amplify small-amplitude oscillations until they become visible on the background of rising outputs (Fig. 6B). The uniform noise with much smaller magnitude  $d = 1.0 \times 10^{-60}$  cannot produce visible amplification of oscillations. However, it significantly increases the rate of growth in neural outputs and shortens the time interval to output saturation (Fig. 6C).

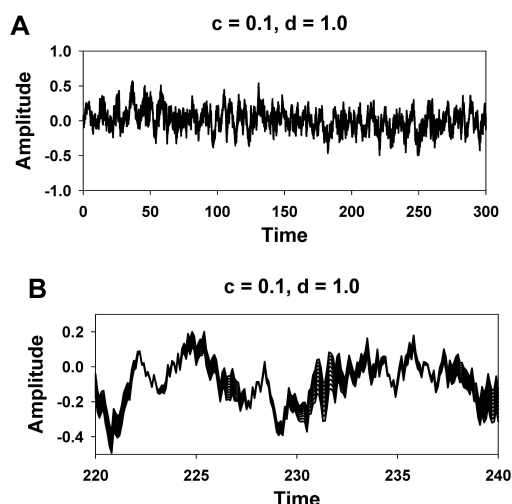


Fig. 7 Neural network outputs under influence of external noise:  $c = 0.1$ ,  $d = 1.0$ , subthreshold case, neural network with asymmetric connections. Panel B shows details of asynchronous activity from panel A

To investigate the effects of connection asymmetry on a Hopfield neural network activity with the applied external uniform noise, we studied behavior of the neural network with asymmetric connections. At subthreshold values of  $c = 0.1$  the neural network produces irregular outputs (Fig. 7A). It is interesting that unlike in corresponding case of fully connected neural network, which generated synchronous irregular oscillations, the neural network with asymmetric connections produces asynchronous outputs (see details in Fig. 7B). This points to the fact that asymmetry in interneuron connections changes synchronization properties of the neural network.

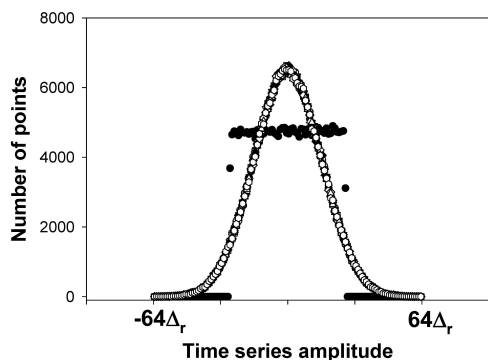


Fig. 8 Normalized amplitude distribution functions of the neural network outputs with the external noise (bell-shaped distributions for all 10 neurons are plotted) and for the amplitudes of external noise (filled circles):  $c = 0.1$ , subthreshold case, neural network with asymmetric connections

The next question is whether the neural network with upper triangular matrix of connection has the same transformation properties, as the fully connected neural network. For this purpose, we calculated amplitude distribution functions for the outputs of each neuron in the neural network with asymmetric connections. Simulation data are shown in Fig. 8. All 10 neurons in the network have bell-shaped normalized amplitude

distribution functions shown by different symbols. For comparison, normalized amplitude distribution function for uniform noise is shown in Fig. 8 by filled circles. It is seen that the asymmetric neural network transforms external uniform noise into irregular neural outputs with bell-shaped distribution functions. However, unlike in case with fully connected neural network, such neural outputs are not synchronized with each other (Fig. 7B).

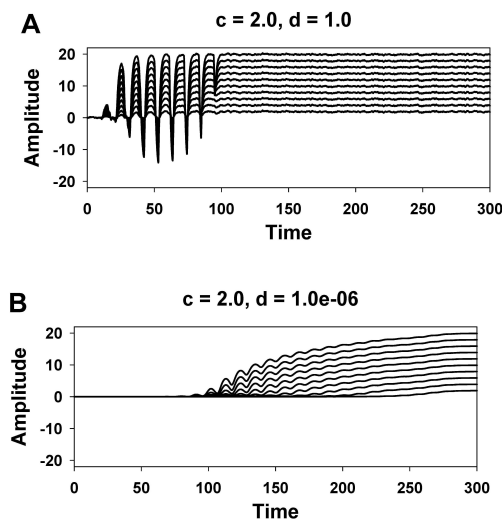


Fig. 9 Activity of the neural network with upper triangular matrix of connections and external noise. Supratherreshold case ( $c = 2.0$ ); external noise amplitudes are  $d = 1.0$  (A) and  $d = 1.0 \times 10^{-6}$  (B).

Finally, we investigated a supratherreshold case of neural activity of the network with asymmetric connections. In this case, the neural outputs possess properties of both symmetric neural network with the applied noise and asymmetric neural network without noise. As in the case of the symmetric network, the noise causes huge amplification of small-amplitude oscillations on the interval where the neural outputs transition to the saturation values ( $d = 1.0$ , Fig. 9A). Different neural outputs saturate at different magnitudes, depending on the number of neural inputs. At smaller values of  $d = 1.0 \times 10^{-6}$ , the amplification of oscillations is to lesser amplitudes (Fig. 9B). The smaller noise amplitude also leads to a longer time interval for the neural outputs to achieve saturation levels.

#### IV. CONCLUSION

We simulated the behavior of an analog Hopfield neural network with time delay. The results of simulations show that the symmetric neural network without noise produces behavior commonly seen in other nonlinear dynamical systems, i. e., the exponential growth of amplitudes until saturation. In asymmetric neural networks, we found an additional unusual type of behavior – an interval of linear growth before saturation. Neural networks with symmetric and asymmetric connections and without external noise demonstrate different synchronization properties. The outputs of the symmetric neural networks are fully synchronous (both in time and in

amplitude), while the asymmetric neural network outputs are synchronized in time only. There are similarities and differences in the effects of the uniform external noise on the behavior of Hopfield neural networks. In subthreshold cases, symmetric and asymmetric neural networks demonstrate different synchronization properties: the outputs of symmetric networks are fully synchronized, while the outputs of asymmetric networks are not synchronous. Both synchronous and asynchronous neural networks transform the uniform amplitude distribution function of the external noise into bell-shaped amplitude distribution functions of the neural outputs. In suprathreshold cases, both neural networks demonstrate huge amplification of the oscillatory component of the neural outputs by the external noise and noise-induced decrease in the time interval for the outputs to achieve their saturation values.

#### REFERENCES

- [1] C.-J. Cheng, T.-L. Liao, and C.-C. Hwang, "Exponential synchronization of a class of chaotic neural networks," *Chaos, Solitons, and Fractals*, vol. 24, pp. 197-206, Apr. 2005.
- [2] C. M. Marcus and R. M. Westervelt, "Stability of analog neural networks with delay," *Phys. Rev. A*, vol. 39, pp. 347-359, Jan. 1989.
- [3] J. Cao, P. Li, and W. Wang, "Global synchronization in arrays of delayed neural networks with constant and delayed coupling," *Phys. Lett. A*, vol. 353, pp. 318-325, May 2006.
- [4] V. E. Bondarenko, "High-dimensional chaotic neural network under external sinusoidal force," *Phys. Lett. A*, vol. 236, pp. 513-519, Dec. 1997.
- [5] V. E. Bondarenko, "Information processing, memories, and synchronization in chaotic neural network with the time delay," *Complexity*, vol. 11, pp. 39-52, Nov.-Dec. 2005.
- [6] V. E. Bondarenko, "A simple neural network model produces chaos similar to the human EEG," *Phys. Lett. A*, vol. 196, pp. 195-200, Dec. 1994.
- [7] V. E. Bondarenko, "Analog neural network model produces chaos similar to the human EEG," *Int. J. Bifurcat. Chaos*, vol. 7, pp. 1133-1140, May 1997.
- [8] V. E. Bondarenko, "Self-organization processes in chaotic neural networks under external periodic force," *Int. J. Bifurcat. Chaos*, vol. 7, pp. 1887-1895, Aug. 1997.
- [9] L. M. Hively, V. A. Protopopescu, and P. C. Gailey, "Timely detection of dynamical change in scalp EEG signals," *Chaos*, vol. 10, pp. 864-875, Dec. 2000.
- [10] V. A. Protopopescu, L. M. Hively, and P. C. Gailey, "Epileptic event forewarning from scalp EEG," *J. Clin. Neurophysiol.*, vol. 18, pp. 223-245, May 2001.

**Kelvin Rozier** received the B.S. degree in mathematics from Georgia State University, Atlanta, GA, in 2011 and is currently working on the PhD degree in mathematics with a concentration in bioinformatics at Georgia State University, Atlanta, GA. Mr. Rozier is a Student Research Assistant in the Department of Mathematics and Statistics at Georgia State University, Atlanta, GA. He has made several presentations at undergraduate research conferences in the field of neural networks. His current research interests include neural networks, dynamic systems, and mathematical music theory.

**Vladimir E. Bondarenko** graduated from Faculty of Physics, Moscow State University (Moscow, Russia) in 1986. In 1990 he obtained a degree Candidate of Science in Physics and Mathematics (PhD analog) from Faculty of Physics, Moscow State University (Moscow, Russia). His major fields of study are plasma physics, polymer science, dynamical systems, ion channel models, neural network models, cardiac cellular and multicellular models. Since graduation in 1986 from Moscow State University, he worked as an Engineer, Junior Researcher, and Researcher in A. L. Mintz Radiotechnical Institute, Moscow, Russia ('86-'94), Researcher and Senior Researcher in the Institute of Biochemical Physics, Moscow, Russia ('94-'98), Postdoctoral Fellow in the University of Pittsburgh, Pittsburgh, PA ('98-'99) and Penn State University, Hershey, PA ('99-'00), Postdoctoral Fellow and Research Assistant Professor in the University of Buffalo, SUNY, Buffalo, NY ('00-'08). Currently he is an Assistant Professor in the Department of Mathematics and Statistics, Georgia State University, Atlanta, GA. He has published 50 papers in peer reviewed journals and a number of papers in conference proceedings. Current research interests include ion channels, neural and cardiac cell models, neural networks, and models of cardiac arrhythmias. Dr. Bondarenko is a member of Biophysical Society and American Heart Association.